

Influence of $s, p-d$ and $s-p$ exchange couplings on exciton splitting in $\text{Zn}_{1-x}\text{Mn}_x\text{O}$

W. Pacuski,^{1,2,*} J. Suffczyński,¹ P. Osewski,¹ P. Kossacki,¹ A. Golnik,¹ J. A. Gaj,^{1,†}
C. Deparis,³ C. Morhain,³ E. Chikoidze,⁴ Y. Dumont,⁴ D. Ferrand,² J. Cibert,² and T. Dietl^{5,1}

¹*Faculty of Physics, University of Warsaw, Hoża 69, PL-00-681 Warszawa, Poland*

²*Institut Néel/CNRS-Université J. Fourier, Boîte Postale 166, F-38042 Grenoble, France*

³*Centre de Recherches sur l'Hétéroépitaxie et ses Applications, CNRS,
rue Bernard Grégory, Parc Sophia Antipolis, F-06560 Valbonne, France*

⁴*Groupe d'Etude de la Matière Condense, CNRS-Université de Versailles, 45, Ave Etats Unis, 78035, Versailles, France*

⁵*Institute of Physics, Polish Academy of Sciences,
al. Lotników 32/46, PL-02-668 Warszawa, Poland*

This work presents results of near-band gap magneto-optical studies on $\text{Zn}_{1-x}\text{Mn}_x\text{O}$ epitaxial layers. We observe excitonic transitions in reflectivity and photoluminescence, that shift towards higher energies when the Mn concentration increases and split nonlinearly under the magnetic field. Excitonic shifts are determined by the $s, p-d$ exchange coupling to magnetic ions, by the electron-hole $s-p$ exchange, and the spin-orbit interactions. A quantitative description of the magnetorefectivity findings indicates that the free excitons A and B are associated with the Γ_7 and Γ_9 valence bands, respectively, the order reversed as compared to wurtzite GaN. Furthermore, our results show that the magnitude of the giant exciton splittings, specific to dilute magnetic semiconductors, is unusual: the magnetorefectivity data is described by an effective exchange energy $N_0(\beta^{(\text{app})} - \alpha^{(\text{app})}) = +0.2 \pm 0.1$ eV, what points to small and positive $N_0\beta^{(\text{app})}$. It is shown that both the increase of the gap with x and the small positive value of the exchange energy $N_0\beta^{(\text{app})}$ corroborate recent theory describing the exchange splitting of the valence band in a non-perturbative way, suitable for the case of a strong $p-d$ hybridization.

PACS numbers: 75.50.Pp, 75.30.Hx, 78.20.Ls, 71.35.Ji

I. INTRODUCTION

It is increasingly clear¹ that the understanding and functionalization of dilute magnetic semiconductors (DMSs) and dilute magnetic oxides (DMOs) has to proceed *via* detailed investigations of spin-dependent couplings between effective mass carriers residing in sp bands and electrons localized on d shells of transition metals. According to a recent model,² a local potential produced by a strong $p-d$ hybridization specific to wide bandgap DMSs and DMOs may give rise to the presence of a hole bound state in the gap, even if the transition metal (TM) ion acts as an isoelectronic impurity. In this strong coupling case, the standard theory, invoking virtual crystal and molecular field approximations to describe exchange splitting of bands, ceases to be valid.² A non-perturbative treatment of the $p-d$ coupling within the generalized alloy theory³ demonstrated that the spin splitting of *extended* valence band states resulting from interactions with randomly distributed magnetic impurities, each acting as a deep hole trap, is reversed and much reduced.² This view was recently supported by *ab initio* computations within an LSDA + U approach for a series of (II,Mn)VI compounds.⁴ It was also suggested⁵ that the developed theoretical framework² explains an anti-crossing-like behavior of bands in mismatched alloys, such as $\text{GaAs}_{1-x}\text{N}_x$, often assigned to the presence of resonant impurity states.⁶

The predictions of the strong coupling model² were experimentally confirmed for wurtzite $\text{Ga}_{1-x}\text{Fe}_x\text{N}$ and $\text{Ga}_{1-x}\text{Mn}_x\text{N}$, where a small and positive value of the ap-

parent $p-d$ exchange energy $N_0\beta^{(\text{app})}$ was inferred from magneto-reflectivity studies of free excitons.^{5,7,8} An unexpectedly small magnitude of $N_0\beta^{(\text{app})}$ was also found in $\text{Zn}_{1-x}\text{Co}_x\text{O}$,⁹ whose sign depended on the assumed ordering of the valence bands on ZnO, a much disputed issue in the physics of this important compound.¹⁰⁻¹⁵

The validity of the model² for the description of $\text{Zn}_{1-x}\text{Mn}_x\text{O}$ has not yet been clarified. Recent transmission experiments indicated the presence of an absorption band in the sub-gap spectral region.^{16,17} In agreement with the strong coupling theory, this additional absorption was considered to originate from photoexcitation of a hole in a Mn bound state and an electron in the conduction band. The corresponding optical cross-section was found to be large enough to shadow internal Mn^{2+} transitions, expected to appear within the same spectral region. The trapping of holes by Mn ions explained also a decay of photoluminescence (PL) intensity with the Mn concentration.

The previous PL study¹⁸ of bound excitons in $\text{Zn}_{1-x}\text{Mn}_x\text{O}$ under an applied magnetic field indicated a much smaller magnitude and a reverse sign of the splitting compared to other II-VI DMSs, in qualitative agreement with the theory.² This view was called into question by results of magnetic circular dichroism (MCD) measurements which indicated that the sign and an overall magnitude of the MCD signal were actually similar to other II-VI DMSs.¹⁷ Moreover, it can be argued that conclusions based on PL results are misleading if magnetic ions act as PL killers. In such a case, if the sample is not perfectly homogenous, the emission comes primarily

from regions with low magnetic ion concentrations and, thus, characterized by a relatively small magnitude of the spin splitting. This problem is not important in the case of reflectivity, whose amplitude is virtually independent of the magnetic ion concentration.

We have, therefore, decided to perform, in addition to the PL and the MCD measurements, reflectivity studies on high quality samples exhibiting sharp excitonic lines. Extensive magnetorefectivity results and their quantitative analysis taking into account excited states as well as both $s, p-d$ and $s-p$ (electron-hole) exchange interactions reported here suggest that the excitons A and B correspond to different valence bands (Γ_7 and Γ_9 , respectively) than in GaN. Furthermore, the findings point to the positive sign and to a reduced magnitude of $\beta^{(\text{app})}$, confirming the applicability of the strong coupling model² for ZnO-based DMSs. We explain mutually opposite polarization of the lowest excitonic lines seen in reflectivity and photoluminescence measurements.

II. SAMPLES AND EXPERIMENTAL

A series of about $1 \mu\text{m}$ thick $\text{Zn}_{1-x}\text{Mn}_x\text{O}$ layers has been grown by molecular beam epitaxy (MBE) and metal-organic vapor phase epitaxy (MOVPE) on sapphire substrates. The c -axis is parallel to the growth direction and the Mn concentrations x , determined by secondary ion mass spectroscopy (SIMS), is 0.14, 0.6, 1.4, and 2.6% for the layers grown by MBE, and 2.5% for the film obtained by MOVPE. A high pressure Xe lamp was employed for reflectivity and transmission experiments. Photoluminescence was excited by a He-Cd laser. Circularly polarized light was analyzed by an achromatic quarter-wave plate and fused silica linear polarizer. A Peltier cooled CCD camera coupled to a 1800 gr/mm grating monochromator was used to record the spectra. The magneto-optical data were collected in the Faraday geometry and with the light incidence normal to the film plane. The sign of circular polarization σ^\pm was checked by a reference measurement of the giant Zeeman splitting of excitons in $\text{Cd}_{1-x}\text{Mn}_x\text{Te}$.

III. RESULTS

A. Zero field spectroscopy

Reflectivity and photoluminescence spectra of diluted $\text{Zn}_{1-x}\text{Mn}_x\text{O}$ ($x = 0.6\%$) are shown in Fig. 1. Several features related to excitonic transitions are seen. In general, three kinds of excitons associated with three closely lying valence bands, are expected in wurtzite semiconductors. They are traditionally referred to as A , B , and C , where the ground state of the exciton A has the lowest and of the exciton C the highest photoexcitation energy. Accordingly, in the reflectivity spectrum collected for the incidence angle of 45 degrees all three 1S excitons A , B ,

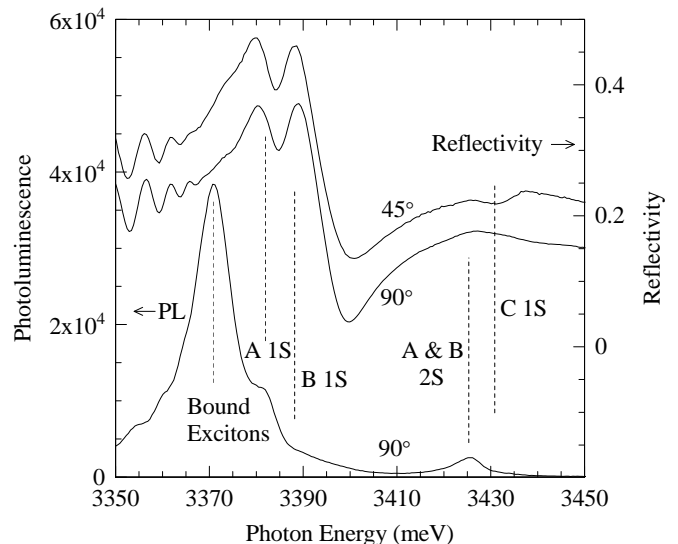


FIG. 1: Reflectivity and photoluminescence of $\text{Zn}_{1-x}\text{Mn}_x\text{O}$ with $x = 0.6\%$ at $T = 1.6 \text{ K}$. The reflectivity is measured with incidence angle of 45 degrees (upper spectrum shifted for clarity) or with normal incidence (middle spectrum). Estimated spectral positions of excitonic lines are indicated.

and C are observed (Fig. 1, topmost spectrum). The $A-B$ splitting is about 7 meV, the $B-C$ splitting is about 45 meV. Due to a weak spin-orbit coupling and optical selection rules no exciton C is observed in the reflectivity spectra obtained with the normal incidence (Fig. 1, middle spectrum). The 2S excitons are much weaker than the 1S excitons and are shifted about 40 meV to higher energies. In the PL spectrum of the same sample (Fig. 1, bottom spectrum), the dominating line, identified as the recombination of a donor bound exciton, is shifted towards lower energies by 11 meV as compared to a weaker line of free exciton A (1S). Emission from the 2S excited states is well visible about 40 meV above the free excitons. Comparing to a reference ZnO sample (not shown) excitonic transitions in $x = 0.6\%$ sample are shifted by 5 meV towards higher energies.

Figures 2(a) and 2(b) show the reflectivity and PL spectra, respectively for samples with different Mn concentrations x . Optical transitions of the A and B excitons are well resolved in the reflectivity spectra for x up to 1.4%. With increasing x the excitonic transitions broaden and shift towards higher energies, in qualitative consistency with previous reports.¹⁷ The same trend is observed for transitions seen in PL (Fig. 2(b)).

The fitting of the reflectivity spectra by the polariton model^{5,9} provides the energy values of the A and B excitons, even in the case of the samples with the highest concentration of magnetic ions $x = 2.6\%$, where relevant lines are rather broad. Figure 3 shows the energy positions of the A and B excitons determined from the spectra presented in Fig. 2(a). The energy of the bound exciton determined from the PL spectra of Fig. 2(b) is also shown. A linear dependence of the energy band gap

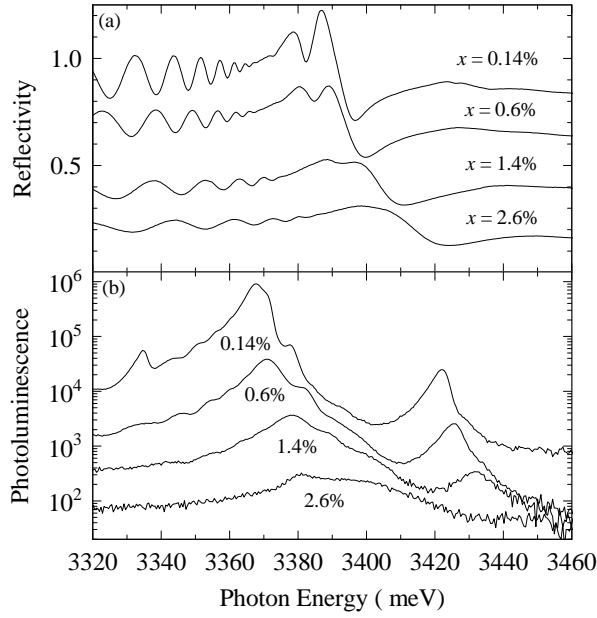


FIG. 2: Reflectivity (a) and photoluminescence (b) spectra collected at 1.6 K for $\text{Zn}_{1-x}\text{Mn}_x\text{O}$ with Mn concentrations 0.14, 0.6, 1.4, and 2.6%. Reflectivity spectra are shifted vertically for clarity. Intensity of photoluminescence spectra decreases by orders of magnitude with increasing the Mn concentration.

on x confirms previous reports on $\text{Zn}_{1-x}\text{Mn}_x\text{O}$,^{16,17,19,20} and is consistent with theoretical expectations for the case of the strong $p-d$ hybridization.² Similar slope for reflectivity and PL (Fig. 3) shows that regions with lower Mn concentration do not dominate the PL spectrum.

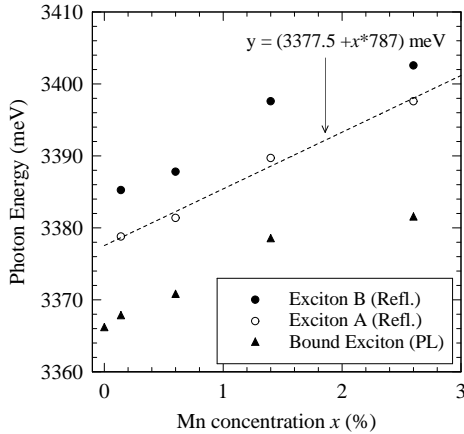


FIG. 3: Exciton energies determined from the spectra shown in Fig. 2, as a function of the Mn concentration x in $\text{Zn}_{1-x}\text{Mn}_x\text{O}$. Empty circles – free exciton A (reflectivity), full circles – free exciton B (reflectivity), triangles – bound exciton (main PL line). The dashed line is a linear fit to the energy of the free exciton A.

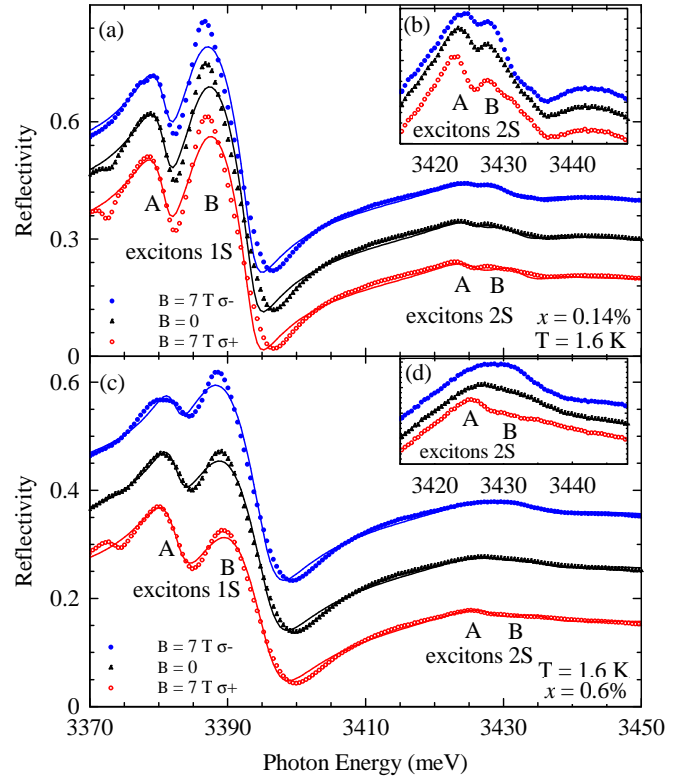


FIG. 4: (color online) Reflectivity spectra (symbols) of $\text{Zn}_{1-x}\text{Mn}_x\text{O}$ with $x = 0.14\%$ (a,b) and $x = 0.6\%$ (c,d). Lines show fits by the polariton model. Features related to 1S and 2S excitons A and B are marked. Spectral region of 2S excitons is plotted in a zoomed Y scale in the insets (b) and (d). Full (empty) circles are related to measurement at σ^- (σ^+) circular polarization and magnetic field $B = 7$ T, triangles to measurement at $B = 0$ T.

B. Magneto-reflectivity

Figure 4 presents reflectivity spectra of samples with $x = 0.14\%$ and 0.6% recorded in the magnetic field $B = 0$ and 7 T for two circular polarizations. A high optical quality of the samples allows us to resolve transitions of 1S as well as of 2S excitonic states, as indicated in the plot.

In order to determine the exact energy positions of excitons from reflectivity spectra, we fit the data employing the polariton model.^{5,9} The model takes into account excitons A and B, their excited states, and transitions to continuum of states through a residual dielectric function. Since the exciton C is not observed, its oscillator strength is assumed to be equal to zero. All excited states are described by a single fitting parameter⁵ (Γ_∞). The importance of the excited states for the interpretation of reflectivity spectra in GaN was pointed out by Stępniewski *et al.*²¹ We find that the inclusion of excited states such as 2S is also crucial for a satisfactory description of reflectivity spectra in the case of ZnO. Interestingly, as clearly evidenced in Fig. 4(a,b) the energy split-

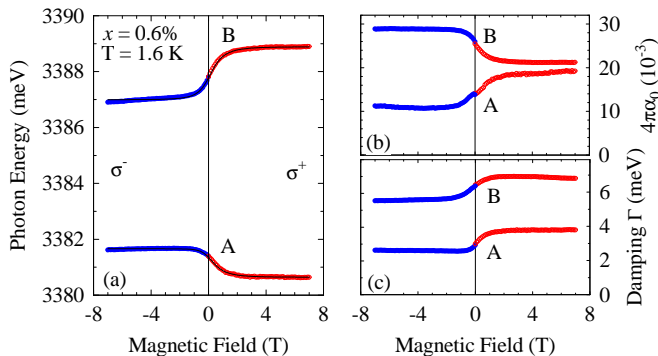


FIG. 5: (color online) Transition energies (a), polarizabilities (b), and damping parameters (c) determined for A and B excitons in $\text{Zn}_{0.994}\text{Mn}_{0.006}\text{O}$ sample. Lines in (a) represent fit with excitonic model, Brillouin function and with parameters given in Table I.

ting between $2S$ A and B excitons is smaller than between $1S$ A and B excitons. This reveals that the magnitude of the electron-hole exchange interaction is much larger in the case of $1S$ excitons.

Examples of experimental and calculated reflectivity spectra are shown in Fig. 4(a,c) and Fig. 6(a). Parameters of the $1S$ excitonic transitions (transition energies, polarizabilities, and damping parameters) obtained from the fit for the sample containing 0.6% of Mn are plotted as a function of the magnetic field in Fig. 5. The analysis of the two circular polarizations of the light shows that both excitons A and B split in the magnetic field. However, in contrast to $\text{Ga}_{1-x}\text{Fe}_x\text{N}^5$ and $\text{Ga}_{1-x}\text{Mn}_x\text{N}^8$ the splitting magnitude is larger in the case of the exciton B (2 meV at saturation) than in the case of the exciton A (1 meV at saturation). Since a larger splitting is expected for the Γ_9 band (derived from the heavy hole $j = 3/2$ band) than for the Γ_7 case, we conclude that the A exciton is associated with the Γ_7 band in ZnO , in contrast to GaN , where the relevant band is Γ_9 . We note that such an ordering has been proposed for ZnO by Thomas¹⁰ and recently confirmed using the analysis of donor bound excitons in ZnO bulk material.^{14,15}

According to the fitting results collected in Fig. 5, the field-induced excitonic shifts are much more pronounced in the σ^+ circular polarization than in the σ^- one. This stems from the presence of an electron-hole exchange interaction that leads to a mixing between A and B excitonic states.^{9,12} When the energy distance between excitons A and B increases (in σ^+), exciton mixing becomes weaker. In contrast, in the case of the σ^- circular polarization, the energy separation between excitons A and B decreases in the magnetic field. This enhances the exciton mixing and the resulting anticrossing behavior, which reduces strongly the field-induced shift of the corresponding excitonic states.

Once determined the exciton energies and their shifts in the magnetic field, we employ the theory of free excitons in wurtzite DMSs^{5,9,22} in order to assess the selec-

E_A	$\tilde{\Delta}_1$	Δ_2	Δ_3	γ	$N_0(\beta^{(\text{app})} - \alpha^{(\text{app})})$
3381.4	51.1	0.5	11.6	2.7	+220

TABLE I: Energies in meV of the ground state exciton A , E_A ; crystal field splitting $\tilde{\Delta}_1$; spin-orbit parameters Δ_2 and Δ_3 ; $s-p$ and $s,p-d$ exchange interactions, γ and $N_0(\beta^{(\text{app})} - \alpha^{(\text{app})})$, respectively describing energies of excitons A and B as a function of the magnetic field in $\text{Zn}_{1-x}\text{Mn}_x\text{O}$ with $x = 0.6\%$.

tion rules and to evaluate the values of relevant parameters for $\text{Zn}_{1-x}\text{Mn}_x\text{O}$. As shown in Table I, the fitting procedure provides the magnitudes of the crystal field splitting $\tilde{\Delta}_1$, spin-orbit parameters Δ_2 and Δ_3 as well as the electron-hole exchange energy γ and a combination of the $s,p-d$ exchange energies, $N_0(\beta^{(\text{app})} - \alpha^{(\text{app})})$, where N_0 is the cation concentration; $\beta^{(\text{app})}$ and $\alpha^{(\text{app})}$ are the apparent $p-d$ and $s-d$ (respectively) exchange integrals describing the splitting of the extended hole and electron states which form the excitons. The presence of antiferromagnetic interactions between the nearest neighbor Mn pairs²³ is taken into account by introducing an effective Mn concentration, $x_{\text{eff}} = x(1-x)^{12}$.

Parameter Δ_2 describes the parallel component of spin-orbit interaction that induces the $A-B$ valence band splitting. According to a common interpretation^{9,13} a positive value of Δ_2 would imply that the order of the valence bands is the same in ZnO and GaN (namely, $\Gamma_9, \Gamma_7, \Gamma_7$). However, in the case of the present study, the value of the $\Delta_2 = 0.5 \pm 1$ meV determined from the fit is very small. As a consequence, the perpendicular component of the spin orbit interaction (Δ_3) governs the valence band ordering. Parameter Δ_3 describes the Γ_7 - Γ_7 valence bands interaction that pushes one of the Γ_7 bands to the top of the valence bands. In the view of the above considerations, the observed valence band ordering is $\Gamma_7, \Gamma_9, \Gamma_7$.

For excitons the situation is more complex. The electron-hole $s-p$ exchange interaction increases the splitting between excitons A and B as compared to valence band distance. Moreover, $s-p$ exchange interaction mixes valence bands within excitonic states. Consequently, the hole in the exciton A originates partially from both Γ_7 and Γ_9 valence bands. However, the main contribution comes from the Γ_7 valence band, rather than from the Γ_9 band, as it would in GaN . The difference in the exciton origin accounts also for a reverse sign and amplitude of the giant Zeeman splitting of the excitons A and B in $\text{Zn}_{1-x}\text{Mn}_x\text{O}$ and $\text{Zn}_{1-x}\text{Co}_x\text{O}$,⁹ compared to $\text{Ga}_{1-x}\text{Fe}_x\text{N}$ and $\text{Ga}_{1-x}\text{Mn}_x\text{N}$.^{5,8} The fitting procedure leads also to $N_0(\beta^{(\text{app})} - \alpha^{(\text{app})}) = +0.22 \pm 0.05$ eV, where the main contribution to the error comes from the uncertainty in the x value.

Positions of A and B excitons obtained from the polaron fit for the case of $\text{Zn}_{1-x}\text{Mn}_x\text{O}$ with higher Mn content, $x = 2.6\%$, are indicated by arrows in Fig. 6. When a mag-

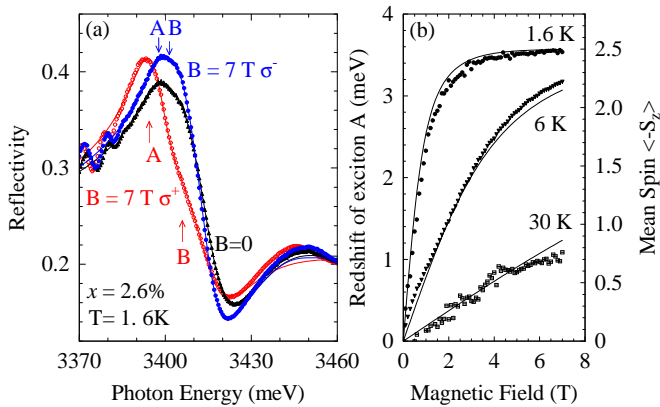


FIG. 6: (color online) (a) Reflectivity spectra (symbols) of $\text{Zn}_{1-x}\text{Mn}_x\text{O}$ with $x = 2.6\%$, measured at $B = 0$ and $B = 7$ T in two circular polarizations at $T = 1.6$ K. Solid lines show fits with the polariton model. Arrows show the determined positions of excitons. (b) Redshift of the exciton A as a function of the magnetic field B , as determined for in $\text{Zn}_{0.974}\text{Mn}_{0.026}\text{O}$ at three temperatures T (left axis). The redshift is compared to the mean spin of Mn^{2+} ions (right axis), given by the paramagnetic Brillouin function $B_{5/2}(T, B)$.

netic field is applied a substantial redshift of the exciton A in the σ^+ polarization is clearly visible even without the polariton fit. Since the low-energy component of the exciton A does not anticross with other excitons, the influence of the electron-hole exchange interaction on its shift is weak. Accordingly, as shown in Figure 6(b), the redshift of the exciton A is directly proportional to the paramagnetic Brillouin function $B_{5/2}(T, B)$, where T is the sample temperature. The data confirm a dominant contribution of the $s, p - d$ exchange interaction to the giant Zeeman splitting and indicate that the spin-spin coupling between next nearest Mn neighbors is weak in $\text{Zn}_{1-x}\text{Mn}_x\text{O}$.

C. Magnetic circular dichroism and photoluminescence

According to the magneto-reflectivity data discussed above, the redshifted component of the lowest exciton line acquires the σ^+ polarization in the presence of a magnetic field. This conclusion is consistent with the sign of MCD signals reported for $(\text{Zn}, \text{Mn})\text{O}$ in the free exciton spectral region.¹⁷ In contrast, the exciton line detected in PL showed a redshift, but exhibited the σ^- polarization.¹⁸ In order to clarify this issue, we have carried out MCD and PL measurements on the same $\text{Zn}_{0.975}\text{Mn}_{0.025}\text{O}$ film. The shape and the sign of the transmission MCD signal (Fig. 7a) are the same as reported previously for $(\text{Zn}, \text{Mn})\text{O}$,^{17,24} and other II-VI DMSs, including $\text{Zn}_{1-x}\text{Co}_x\text{O}$.^{9,25}

A comparison of Figs. 7(a) and 7(b) indicates that the spectral position of the PL line is shifted towards lower energies with respect to the MCD maximum. This can be

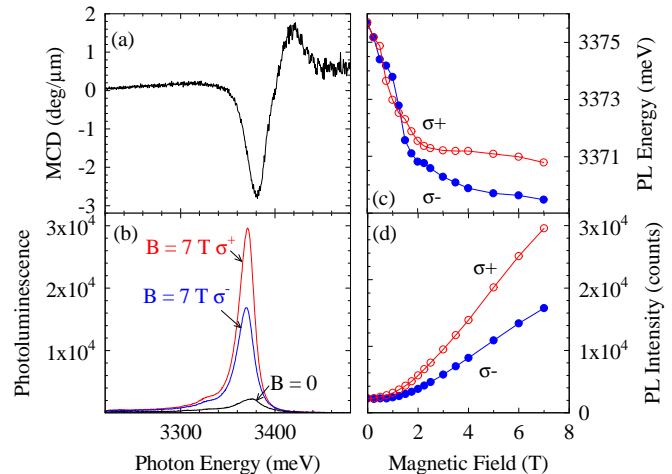


FIG. 7: (color online) Magnetic Circular Dichroism (MCD) in 6 T (a) and photoluminescence (PL) spectra measured at $B = 0$ and $B = 7$ T in two circular polarizations (b) for $\text{Zn}_{1-x}\text{Mn}_x\text{O}$ with 2.5% of Mn at $T = 1.6$ K. Spectral position (c) and amplitude (d) of the PL peak vs. magnetic field.

expected as transmission measurements probe primarily free excitons while PL involves mainly excitons bound to residual impurities. The incorporation of magnetic ions leads to a significant quenching of the excitonic PL intensity in these systems, particularly if magnetic ions can absorb the excitation energy or trap photocarriers. However, as shown in Figs. 7(b) and 7(d) the intensity of the PL lines in both polarizations increases nonlinearly with the magnetic field. As a consequence, total PL intensity increases by an order of magnitude when magnetic field increases from 0 to 7 T, as shown in Fig. 7(d). This indicates that applying a magnetic field limits the impact of non-radiative processes on the emission from the excitonic states. A similar effect was reported for $\text{Zn}_{1-x}\text{Mn}_x\text{Se}$,²⁶ and explained by spin polarization of carriers and Mn^{2+} ions, which blocked the transfer of the excitation to Mn ions.

The energy positions of the PL lines are depicted in Fig. 7(c) as a function of the magnetic field. The strongest line exhibits a nonlinear redshift and σ^+ polarization. The redshift starts to saturate around $B = 2$ T and attains 5 meV at 7 T. As discussed in the previous section, a similar magnitude of the redshift is found for the ground state exciton A in the reflectivity measurements in the same polarization. Interestingly, in addition to the PL line in the σ^+ polarization, a somewhat weaker PL line emerges at lower photon energies in the σ^- polarization. Actually, in the previous PL studies¹⁸ the lowest exciton line did also exhibit a redshift and the σ^- polarization in the presence of a magnetic field.

As discussed in Sec. III B, the electron-hole exchange contributes significantly to the splitting between the A and B free excitons in ZnO . The influence of the electron-hole exchange is much weaker in the case of bound excitons than in the case of free excitons. Thus, the A - B

splitting is much smaller in the case of bound excitons.²⁷ Actually, we show below (next part and Fig. 8) that the Zeeman shift of the bound excitons can be described assuming no contribution of the electron-hole exchange, as in the case of an acceptor-bound or donor bound exciton. Moreover, the magnetic field induced splitting of the B exciton, originating from the heavy-hole-like Γ_9 band, is larger than (and opposite in sign to) the splitting of the exciton A , which is associated with the Γ_7 band. The opposite circular polarization of the lowest line in the excitonic reflectivity and PL spectra observed at higher magnetic fields suggests therefore that a difference of binding energies of the A and B excitons is comparable to the relative energy distance between valence bands from which they originate. When A and B excitons separation energy at zero magnetic field is negligible, their relative order at magnetic field is governed by the difference of the respective shifts induced by the $s, p - d$ interaction. To sum up, at low magnetic fields, the A and B excitonic lines are too broad (FWHM of ~ 20 meV) to be resolved. At higher magnetic fields, Γ_7 -related exciton A is observed in σ^+ polarization and Γ_9 -related exciton B is observed in σ^- polarization.

Typically, thermalization processes lead to a stronger emission from a lower energy state. It is not the case of the present study: the higher energy PL component (σ^+) exhibits a stronger intensity. We explain this observation in terms of the mechanism of the bound exciton formation. Prior to any bound state formation photocreated holes relax to the lowest Γ_7 valence band (order determined from reflectivity results for free carriers). Next, they form the corresponding bound excitons. This results in the strong σ^+ polarized emission. However, some excitons change their symmetry and transfer to a bound state involving a Γ_9 related hole, being in the magnetic field the lowest bound exciton energy state. Radiative recombination of these excitons results in σ^- polarized emission. Its intensity is governed by the ratio of Γ_7 related exciton formation and recombination and Γ_7 to Γ_9 excitonic transfer rate. The stronger emission in σ^+ than in σ^- polarization indicates that excitonic transfer rate from Γ_7 band to Γ_9 band is relatively small.

IV. EVALUATION OF THE $p - d$ EXCHANGE INTEGRAL

In order to evaluate the magnitude of the $p - d$ exchange energy for $\text{Zn}_{1-x}\text{Mn}_x\text{O}$ we have collected in Fig. 8 the determined redshifts of the exciton A and the blueshifts of the exciton B at magnetization saturation (low temperatures and high magnetic fields), as a function of the Mn concentration. The redshifts of the PL lines are also shown. Taking into account possible errors in the energy and Mn content determination, the relative accuracy is of the order of 20% in the case of both axes. Theoretical lines in Fig. 8 represent the expected energy shift for an exciton associated with the heavy-hole-like Γ_9

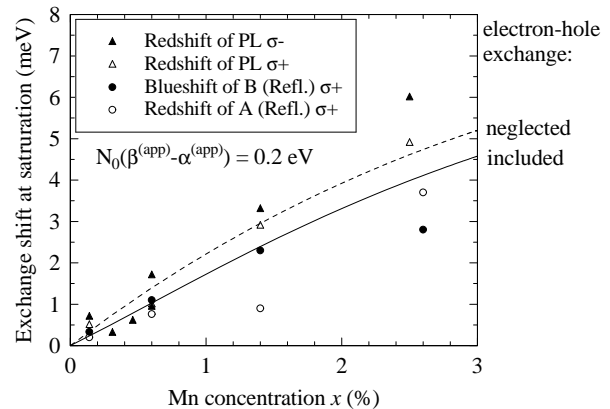


FIG. 8: Shift of exciton energies observed in reflectivity and photoluminescence measurements on $\text{Zn}_{1-x}\text{Mn}_x\text{O}$ plotted as a function of the Mn concentration x . The shifts are determined at saturation of the Mn spin polarization: the redshift of the exciton A by using reflectivity in the σ^+ polarization (empty circles); the blueshift of the exciton B in the σ^+ circular polarization by using reflectivity (full circles); the redshift of the bound exciton from PL measurements in the σ^- polarization (full triangles) and in the σ^+ polarization (empty triangles). PL data for three diluted samples are taken from Ref. 18. Solid line represents the value of the shift calculated for the heavy-hole-like Γ_9 band assuming $N_0(\beta^{(\text{app})} - \alpha^{(\text{app})}) = +0.2$ eV, and is more suitable for the exciton B . Dashed line corresponds to the calculation with the neglected electron-hole exchange interaction and is more suitable for bound excitons seen in the PL, σ^- polarization.

band for which the shift is larger than for the one linked to Γ_7 band, assuming $N_0(\beta^{(\text{app})} - \alpha^{(\text{app})}) = +0.2$ eV, $S = 5/2$, and $x_{\text{eff}} = x(1 - x)^{12}$. The solid (dashed) line is obtained taking into account (neglecting) the electron-hole exchange interaction. As seen, the exchange shift determined from the reflectivity (the PL) measurements is reasonably well described by the solid (dashed) line. This is expected since the electron-hole interaction affects much less bound excitons which are observed in the PL.

Taking the determined value of $N_0(\beta^{(\text{app})} - \alpha^{(\text{app})}) = +0.2 \pm 0.1$ eV and assuming a standard value of $N_0\alpha^{(\text{app})} = +0.3 \pm 0.1$ eV,^{4,28,29} we obtain the $p - d$ exchange energy $N_0\beta^{(\text{app})} = +0.5 \pm 0.2$ eV. If our assignment of the valence band order were incorrect, the resulting value of the $N_0\beta^{(\text{app})}$ would be $N_0\beta^{(\text{app})} = +0.1 \pm 0.2$ eV. We note that the latter value includes zero and negative values within the uncertainty limits. We can estimate the upper limit of the absolute value of the $p - d$ exchange integral $|N_0\beta^{(\text{app})}| < 0.7$ eV.

V. CONCLUSIONS

The giant Zeeman splitting of free excitons has been observed in magneto-reflectivity experiment performed on $\text{Zn}_{1-x}\text{Mn}_x\text{O}$ samples with the Mn concentration x

ranging from 0.14% to 2.6%. In a view of our findings, $\text{Zn}_{1-x}\text{Mn}_x\text{O}$ appears in many aspects to be a typical II-VI DMS: its magnetization is well described by the paramagnetic Brillouin function, circular polarization of the giant Zeeman effect and, thus, the sign of the MCD, are the same as in, *e. g.*, $\text{Cd}_{1-x}\text{Mn}_x\text{Te}$. Although the incorporation of Mn degrades optical quality of the crystal, excitonic transitions are visible in reflectivity and photoluminescence even in the case of samples with a relatively high concentration of magnetic ions. The most important difference is that the overall amplitude of the exciton splitting is one order of magnitude smaller than the one expected for the value of the $p-d$ exchange energy suggested by the Schrieffer-Wolf theory,^{29,30} $N_0\beta = -3.1 \pm 0.1$ eV or implied by x-ray spectroscopy, $N_0\beta = -3.0$ eV.³¹ By a quantitative interpretation of the reflectivity spectra, it has been possible to find out how to link these puzzling results to a structure of the valence band in ZnO and to the strong $p-d$ hybridization, expected for materials with the short anion-cation distance.

More specifically, experimental results and their interpretation presented here for $\text{Zn}_{1-x}\text{Mn}_x\text{O}$ and earlier for $\text{Zn}_{1-x}\text{Co}_x\text{O}$,⁹ $\text{Ga}_{1-x}\text{Mn}_x\text{N}$,^{7,8} and $\text{Ga}_{1-x}\text{Fe}_x\text{N}$,⁵ lead to several conclusions concerning exciton magnetospectroscopy and properties of wide band-gap wurtzite DMSs.

First, a meaningful determination of exciton energies from magneto-reflectivity spectra requires the application of the polariton model that incorporates optical transitions to excitonic excited states and band continuum.

Second, the determined free exciton energies as a function of the magnetic field indicate that the giant Zeeman splitting is larger for the exciton *B* than for the exciton *A* in (Zn,TM)O. This means that the exciton *B* is associated with the heavy-hole-like Γ_9 valence band. This is in contrast to (Ga,TM)N, where a giant splitting is larger

for the exciton *A*, in agreement with the notion that the heavy-hole from the Γ_9 valence band contributes to the ground state exciton *A* in GaN.

Third, quantitative description of excitonic splitting and selection rules requires the model containing the spin-orbit coupling as well as the $s, p-d$ and $s-p$ exchange interactions.

Fourth, the obtained results point to the ferromagnetic character and the small magnitude of the apparent $p-d$ exchange energy, $N_0\beta^{(\text{app})} = +0.5 \pm 0.2$ eV, in $\text{Zn}_{1-x}\text{Mn}_x\text{O}$. These findings, and similar ones for $\text{Zn}_{1-x}\text{Co}_x\text{O}$,⁹ $\text{Ga}_{1-x}\text{Mn}_x\text{N}$,^{7,8} and $\text{Ga}_{1-x}\text{Fe}_x\text{N}$,⁵ substantiate the model predicting the reversed sign and reduced magnitude of the splitting of extended valence band states once the potential produced by individual magnetic ions is strong enough to bind a hole.²

Finally, we comment on consequences of our findings for the search for the hole-mediated ferromagnetism in oxide and nitride DMSs. As already noted,² a significant contribution of the $p-d$ hybridization to the hole binding energy shifts the insulator-to-metal transition to higher hole concentrations, making the conditions for the hole delocalization, a necessary ingredient for the operation of the $p-d$ Zener mechanism of ferromagnetism, difficult to achieve.

Acknowledgments

The work was supported by the EC through the FunDMS Advanced Grant of the European Research Council (FP7 "Ideas") and Polish public funds in years 2010-2013 (Polish MNiSW project Iuventus Plus and Polish NCBiR project LIDER). We thank Roman Stepniewski, Alberta Bonanni, and Hideo Ohno for valuable discussions at various stages of this work.

* Electronic address: Wojciech.Pacuski@fuw.edu.pl

† Deceased.

¹ T. Dietl, *Nature Mat.* **9**, 965 (2010).

² T. Dietl, *Phys. Rev. B* **77**, 085208 (2008).

³ J. Tworzydło, *Phys. Rev. B* **50**, 14591 (1994).

⁴ T. Chanier, F. Viot, and R. Hayn, *Phys. Rev. B* **79**, 205204 (2009).

⁵ W. Pacuski, P. Kossacki, D. Ferrand, A. Golnik, J. Cibert, M. Wegscheider, A. Navarro-Quezada, A. Bonanni, M. Kiecana, M. Sawicki, and T. Dietl, *Phys. Rev. Lett.* **100**, 037204 (2008).

⁶ W. S. J. Wu and W. Walukiewicz, *Semicond. Sci. Technol.* **17**, 860 (2002).

⁷ W. Pacuski, D. Ferrand, J. Cibert, J. A. Gaj, A. Golnik, P. Kossacki, S. Marcet, E. Sarigiannidou, and H. Mariette, *Phys. Rev. B* **76**, 165304 (2007).

⁸ J. Suffczyński, A. Grois, W. Pacuski, A. Golnik, J. A. Gaj, A. Navarro-Quezada, B. Faina, T. Devillers, and A. Bo-

nanni, *Phys. Rev. B* **83**, 094421 (2011).

⁹ W. Pacuski, D. Ferrand, J. Cibert, C. Deparis, J. A. Gaj, P. Kossacki, and C. Morhain, *Phys. Rev. B* **73**, 035214 (2006).

¹⁰ D. G. Thomas, *J. Phys. Chem. Solids* **15**, 86 (1960).

¹¹ D. C. Reynolds, D. C. Look, B. Jogai, C. W. Litton, G. Cantwell, and W. C. Harsch, *Phys. Rev. B* **60**, 2340 (1999).

¹² B. Gil, *Phys. Rev. B* **64**, 201310 (2001).

¹³ W. R. Lambrecht, A. V. Rodina, S. Limpijumng, B. Segall, and B. K. Meyer, *Phys. Rev. B* **65**, 075207 (2002).

¹⁴ M. R. Wagner, J.-H. Schulze, R. Kirste, M. Cobet, A. Hoffmann, C. Rauch, A. V. Rodina, B. K. Meyer, U. Röder, and K. Thonke, *Phys. Rev. B* **80**, 205203 (2009).

¹⁵ L. Ding, B. K. Li, H. T. He, W. K. Ge, J. N. Wang, J. Q. Ning, X. M. Dai, C. C. Ling, and S. J. Xu, *J. Appl. Phys.* **105**, 053511 (2009).

- ¹⁶ M. Godlewski, A. Wąsiakowski, V. Ivanov, A. Wójcik-Głodowska, M. Lukaszewicz, E. Guziejewicz, R. Jakiela, K. Kopalko, A. Zakrzewski, and Y. Dumont, *Optical Materials* **32**, 680 (2010).
- ¹⁷ C. A. Johnson, K. R. Kittilstved, T. C. Kaspar, T. C. Droubay, S. A. Chambers, G. M. Salley, and D. R. Gamelin, *Phys. Rev. B* **82**, 115202 (2010).
- ¹⁸ E. Przeździecka, E. Kamińska, M. Kiecana, M. Sawicki, L. Kłopotowski, W. Pacuski, and J. Kossut, *Solid State Commun.* **139**, 541 (2006).
- ¹⁹ T. Fukumura, Z. Jin, A. Ohtomo, H. Koinuma, and M. Kawasaki, *Appl. Phys. Lett.* **75**, 3366 (1999).
- ²⁰ E. Chikoidze, Y. Dumont, F. Jomard, D. Ballutaud, P. Galtier, O. Gorochov, and D. Ferrand, *J. Appl. Phys.* **97**, 10D327 (2005).
- ²¹ R. Stepniewski, A. Wyszomolek, M. Potemski, K. Pakuła, J. M. Baranowski, I. Grzegory, S. Porowski, G. Martinez, and P. Wyder, *Phys. Rev. Lett.* **91**, 226404 (2003).
- ²² W. Pacuski, Optical spectroscopy of wide-gap diluted magnetic semiconductors, in *Introduction to the Physics of Diluted Magnetic Semiconductors*, edited by J. A. Gaj and J. Kossut, Springer Series in Materials Science Vol. 144, pp. 37–63, 2010.
- ²³ S. Kolesnik, B. Dabrowski, Z. Wiren, H. Kepa, T. Giebul-towicz, C. Brown, J. Leao, and J. Furdyna, *J. Appl. Phys.* **99** (2006).
- ²⁴ K. Ando, H. Saito, Z. Jin, T. Fukumura, M. Kawasaki, Y. Matsumoto, and H. Koinuma, *J. Appl. Phys.* **89**, 7284 (2001).
- ²⁵ K. Ando, H. Saito, Z. Jin, T. Fukumura, M. Kawasaki, Y. Matsumoto, and H. Koinuma, *Appl. Phys. Lett.* **78**, 2700 (2001).
- ²⁶ S. Lee, M. Dobrowolska, and J. K. Furdyna, *Phys. Rev. B* **72**, 075320 (2005).
- ²⁷ B. K. Meyer, J. Sann, S. Eisermann, S. Lautenschlaeger, M. R. Wagner, M. Kaiser, G. Callsen, J. S. Reparaz, and A. Hoffmann, *Phys. Rev. B* **82**, 115207 (2010).
- ²⁸ T. Andrearczyk, J. Jaroszyński, G. Grabecki, T. Dietl, T. Fukumura, and M. Kawasaki, *Phys. Rev. B.* **72**, 121309(R) (2005).
- ²⁹ R. Beaulac and D. R. Gamelin, *Phys. Rev. B* **82**, 224401 (2010).
- ³⁰ J. Blinowski, P. Kacman, and T. Dietl, Kinetic exchange vs. room temperature ferromagnetism in diluted magnetic semiconductors, in *Spintronics*, edited by T. Klemmer, J. Sun, A. Fert, and J. Bass, Materials Research Society Symposium Proceedings Vol. 690, pp. 109–114, 2002.
- ³¹ J. Okabayashi, K. Ono, M. Mizuguchi, M. Oshima, S. Gupta, D. Sarma, T. Mizokawa, A. Fujimori, M. Yuri, C. Chen, T. Fukumura, M. Kawasaki, and H. Koinuma, *J. Appl. Phys.* **95**, 3573 (2004).